Two-magnon Raman scattering in a spin density wave antiferromagnet

Friedhelm Schönfeld*, Arno P. Kampf, Erwin Müller-Hartmann

Institut für Theoretische Physik, Universität zu Köln, Zülpicher Str. 77, D-50937 Köln, Germany

Abstract

We present the results for a model calculation of resonant two-magnon Raman scattering in a spin density wave antiferromagnet. The resonant enhancement of the two-magnon intensity is obtained from a microscopic analysis of the photon–magnon coupling vertex. By combining magnon–magnon interactions with 'triple resonance' phenomena in the vertex function the resulting intensity line shape is found to closely resemble the measured two-magnon Raman signal in antiferromagnetic cuprates.

Keywords: Raman scattering; Two-magnon Raman scattering; Spin density wave

The analysis of the two-magnon Raman intensity has proven to be a valuable tool for probing the collective magnetic excitations in the parent compounds of high-T_c superconductors. In order to address the experimentally observed asymmetric and broad B_{1g} spectrum and the resonant dependence of the intensity on the incoming light frequency we perform a model calculation based on the spin density wave (SDW) state of the single band Hubbard model at half-filling. We show that the frequency dependence of the photon–magnon vertices offers a consistent explanation for the two-magnon data.

Following a diagrammatic formulation [1], we derive the two-magnon intensity from the diagram for the Raman amplitude F shown in Fig. 1 (for details see Ref. [2]). Taking a cut across the two magnon lines with respect to the transferred photon frequency $i\omega_t$ translates into

$$I(\Delta\omega) = \frac{1}{2\pi i} [F(i\omega_t \rightarrow \Delta\omega + i\delta)$$
$$-F(i\omega_t \rightarrow \Delta\omega - i\delta)]. \quad (1)$$

* Corresponding author.

The Raman intensity is proportional to $I(\Delta\omega)$ which is evaluated in the $T \rightarrow 0$ limit. For the calculation of the Raman amplitude F we evaluate the dynamic susceptibility for the transverse spin fluctuations in the SDW state within RPA approximation [3]. In the strong coupling limit the most relevant photon–magnon vertex which enters the vertex function V is shown in Fig. 2. The vertices are derived from the kinetic part of the Hubbard Hamiltonian in the presence of the weak electromagnetic photon field. Final state magnon–magnon interactions are included in the renormalized vertex function Γ [4].

For brevity we focus here on the experimentally relevant resonant case, $(\omega_i - 2\Delta) \sim J$, where ω_i and Δ are the photon frequency and the SDW energy gap, respectively. The exchange coupling J equals $4t^2/U$ for $U \gg t$, t is the hopping amplitude. We find a strong resonance to arise from a scattering process that is contained within the rhomb-shaped vertex diagram (Fig. 2). In this process the photon excited particle–hole pair decays into a particle–hole pair with lower energy by the creation of two magnons
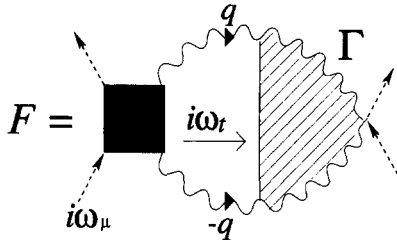
Fig. 1. General diagram for the Raman amplitude of two-magnon scattering. The dashed lines represent the incoming and out-going photons and the wiggly lines the magnon propagators. $i\omega_\mu$ and $i\omega_t$ are the incoming and the transferred frequencies, respectively. The vertex V contains the bare microscopic photon magnon coupling while the renormalized vertex Γ contains in addition magnon–magnon interactions.
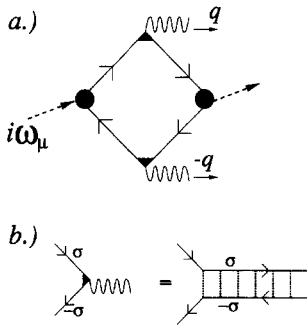

Fig. 2. (a) Dominant contribution to the effective vertex function for the photon–magnon coupling. The solid, dashed, and wiggly lines denote the SDW c-fermion, the photon, and the magnon propagator, respectively. The spin labeling of the fermion lines has been omitted, it is explicitly indicated in (b). The solid circle represents the bare photon–electron coupling, the filled triangle represents the electron–magnon coupling where the magnons are contained in the particle–hole ladder series as shown in (b).

with zero total momentum. Finally, the particle and the hole recombine under emission of the outgoing photon. The strong resonant enhancement of the corresponding vertex function $V_\diamond^R$ (Fig. 2) results from the possible simultaneous vanishing of its three energy denominators and has therefore been termed a 'triple resonance' in Ref. [5]. The numerical analysis of the triple resonance conditions yields that for an intermediate range of incoming photon frequencies the divergence of $V_\diamond^R$ occurs for $\Delta\omega$ near $4J$, where $\Delta\omega$ is the photon frequency shift. The divergence turns into a strong enhancement, if we model quasi-particle lifetime effects from residual interactions between the
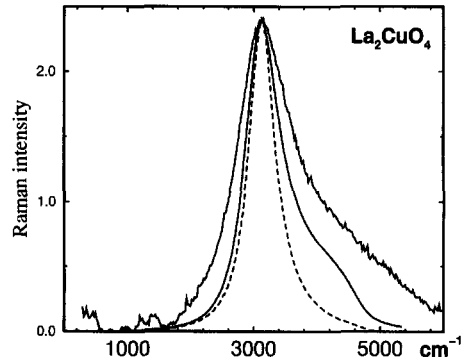

Fig. 3. Raman scattering intensity in arbitrary units in B_{1g} geometry in the non-resonant case (dashed line) and in the resonant case as calculated from Eq. (2) with $(\omega_i - 2\Delta) = 3.6\,J$ for a lattice with 100×100 sites. For the two-magnon term an imaginary broadening of $i\delta = i0.09\,J$ was used in the frequency denominators, while the vertex part was evaluated with $\delta = 0.4\,J$. The jagged line displays the experimental spectrum of La_2CuO_4 taken at room temperature with a laser frequency of $\omega_i = 2.55$ eV [6]. As in Ref. [7] a background was substracted from the Raman data. For comparison with the data the magnetic energy scale was set to $J = 1200$ cm^{-1} and the peak intensities were scaled to coincide.

SDW quasi-particles by adding a finite imaginary part to the energy denominators of the triple resonant vertex function.

In order to solve the Bethe-Salpeter equation for the renormalized vertex function Γ with a triple resonance photon–magnon vertex V^R we have singled out the dominant symmetry-channel, i.e. $\tilde{V}_A^R(q, \omega_i, \Delta\omega) = g(\omega_i, \Delta\omega)\,\gamma_q^d$, with $\gamma_q^d = \frac{1}{2}(\cos q_x - \cos q_y)$, and find the resonant B_{1g} Raman intensity in the form

$$I_{B_{1g}}(\Delta\omega) \propto |g(\omega_i, \Delta\omega)|^2\, I_{B_{1g}}^0(\Delta\omega) . \tag{2}$$

In this way $I_{B_{1g}}$ factorizes into a triple resonance vertex part from the photon magnon coupling and the two-magnon intensity $I_{B_{1g}}^0$.

The resulting line shape is dominated by the two-magnon peak but its high energy shoulder results solely from the triple resonance enhancement in the photon–magnon vertex function. The comparison to the experimental spectrum of La_2CuO_4 taken from Ref. [6] is shown in Fig. 3. The calculated line shape agrees fairly well with the experimental data not only for La_2CuO_4, as shown, but also for the double-layer compound $YBa_2Cu_3O_6.1$ [8]. Besides the high energy shoulder other experimental features like the photon frequency depedence of the intensity line

shape [8] and the existence of *two* separate resonance frequencies both well above the energy gap 2Δ, find a natural explanation as well by the interplay between the two-magnon peak and the triple resonance.

Since we neglected the effects of magnon–phonon and magnon–magnon interactions and also the contribution from four-magnon and higher order scattering processes in our work, the sharper peak of the calculated Raman intensity in comparison to the data is expected on physical grounds.

In conclusion, we found that the combination of resonant transitions between the SDW quasi particle bands and magnon pair excitations provides a microscopic basis for understanding the resonant Raman scattering experiments on cuprate antiferromagnets.

References

[1] A. Kawabata, J. Phys. Soc. Japan 30 (1971) 68.
[2] M.V. Klein, Phys. Rev. B 24 (1981) 4208.
[3] J.R. Schrieffer, X.G. Wen and S.C. Zhang, Phys. Rev. B 39 (1989) 11663.
[4] F. Schönfeld, A.P. Kampf and E. Müller-Hartmann, Z. Phys. B 102 (1997) 25.
[5] A.V. Chubukov and D.M. Frenkel, Phys. Rev. Lett. 74 (1995) 3057; Phys. Rev. B 52 (1995) 9760.
[6] P.E. Sulewski, P.A. Fleury and K.B. Lyons, Phys. Rev. B 41 (1990) 225.
[7] R.R.P. Singh, P.A. Fleury and P.E. Sulewski, Phys. Rev. Lett. 62 (1989) 2736.
[8] G. Blumberg, P. Abbamonte, M.V. Klein, L.L. Miller, W.C. Lee, D.M. Ginsberg and A. Zibold, Phys. Rev. B 53 (1996) R11930.